Dalton Transactions

Accepted Manuscript

ROYAL SOCIETY OF CHEMISTRY

www.rsc.org/dalton

Dalton Transaction

ARTICLE

Influence of extreme conditions on formation and structures of caesium uranium (VI) arsenates

autuniteReceived 00th September 20xx,
Accepted 00th September 20xx

DOI: 10.1039/x0xx00000x

www.rsc.org/

Na Yu[1], Philip Kegler[1], Vladislav V. Klepov[2], Jakob Dellen[1], Hartmut Schlenz[1], Eike Langer[1], Dirk Bosbach[1], and Evgeny V. Alekseev[1,3]*

Four new uranyl arsenates, $Cs_2[(UO_2)(As_2O_7)]$ (**1**), α-$Cs[(UO_2)(HAs_2O_7)]$ (**2**), β-$Cs[(UO_2)(HAs_2O_7)]$ (**3**), $Cs[(UO_2)(HAs_2O_7)]\cdot 0.17H_2O$ (**4**), were synthesized by high-temperature/high pressure (HT/HP) reactions at 900 °C and 3 GPa. These phases were subsequently characterised structurally as well as chemically. We demosntrated that compound **1** also can be obtained at ambient pressure. Compounds **1**, **2**, and **4** are based on two-dimensional (2D) anionic layers with two different topological types. The layers own a similar composition, $[(UO_2)(As_2O_7)]^{2-}$ in **1** and $[(UO_2)(HAs_2O_7)]^{-}$ in **2**, and **4**. However, the presence of hydrogen in **2** and **4** leads to a change of coordination modes of the pyroarsenate groups. There are additional 0.17 H_2O molecules per formula unit in **4**, which causes slight distortions of the layers in **4**. All these layers can be simplified to a common net, which is typical for autunite-like layered compounds. The compound **3** is a polymorph of compound **2**, but the structural arrangements in those two are significantly different. The structure of **3** is based upon a three-dimensional (3D) framework, in which UO_7 is coordinated by arsenate groups in order to form uranyl anion sheets, and UO_6 is located within the interlayers. Bond valance analysis proved the presence of OH^- groups in compounds **2**, **3**, and **4**, respectively, and water molecules in **4**. The Raman analyses enabled the study of the local environments of the arsenate and the uranyl groups within the investigated phases, respectively. It turned out, that the applied HT/HP synthesis method strongly effects the crystal chemistry as well as the observed structural features of all obtained compounds.

Introduction

Actinide chemistry plays an important role within the nuclear fuel cycle and for the management of nuclear waste.[1-5] Several previous studies reported that phosphates could be potentially used as ceramic materials for hosting of tri- and tetravalent actinides.[6-10] Despite the interest on uranium phosphate compounds, data on uranium arsenates, which should exhibit similar properties to phosphate analogues, are barely reported. A deeper knowledge on uranium phosphates and arsenates can be a benefit for the purpose of a better understanding of the structures and the behaviour of uranium and other early actinides in nature, which is also important for the safe management of nuclear waste.

From the fundamental point of view, the structural chemistry of actinides phosphates and arsenates is extremely flexible, due to the complex coordination environment of An-O polyhedra and *T*-O (*T* = P, As) anionic groups.[11,12] The actinides in tetra-valence states (An^{4+}) can achieve high coordination numbers in oxo-phosphate and oxo-arsenate compounds.[13,14] Thus, An^{4+} phosphates and arsenates show a fascinating diversity in their structural chemistry.[15-18] The crystal chemistry of actinides in hexa-valence state (An^{6+}) is dominated by 2D sheets, simply because they are based on linear actinyl cations (AnO_2^{2+}), that own two terminal oxygen atoms preventing 3D linkages.[19,20]

As it is well-known, synthesis conditions do have a strong influence on phase formation in actinide chemistry.[21-23] For instance, pressure is a very important factor in natural as well as in synthetic systems. A major effect of pressure is the reduction of the molar volume (–ΔV), which in turn could lead to a compression of the electron shells of the atoms and can therefore lead to changes of coordination environments, to the formation of new chemical bonds and hence to phase transitions. Due to safety issues regarding the handling of radioactive materials, we are currently very limited in our knowledge on the influence of pressure on actinide bearing compounds. Recently we applied a high-temperature/high-pressure (HT/HP) synthetic method in order to study the U – As – Cs oxo-system, and the first example of a mixed valence As^{3+}/As^{5+} thorium compound $Th(As^{III}_4As^{V}_4O_{18})$ was obtained[24]. Uranium, comparably to thorium, demonstrates more complex behaviour due to possible oxidation state variations from +2 to +6. Such diversity affects the coordination chemistry of uranium and the complexity of uranium bearing compounds.[12, 25, 26]

[a] *Institute for Energy and Climate Research (IEK-6), Forschungszentrum Jülich GmbH, 52428 Jülich, Germany.*
[b] *Department of Chemistry, Samara State University, 443011 Samara, Russia.*
[c] *Institut für Kristallographie, RWTH Aachen University, 52066 Aachen, Germany.*
† Footnotes relating to the title and/or authors should appear here.
Electronic Supplementary Information (ESI) available: Syntheses of single crystals of $Cs_2[(UO_2)(As_2O_7)]$ at ambient pressure and high temperature conditions, EDS measuring sample image and results, Bond-valence sums (BVS), and crystallographic data in CIF See DOI: 10.1039/x0xx00000x

Besides, the influence of extreme conditions on the formation of uranyl compounds has been studied quite barely. Such studies mainly were performed at relatively low pressures and temperatures.[27-32] In this report we present the results of the U – As – Cs oxo-system investigations, aimed to explore the synthetic and coordination chemistry of uranium under extreme (HT/HP) conditions. Herein, we obtained four new uranium(VI) arsenates, $Cs_2[(UO_2)(As_2O_7)]$ (**1**), α-$Cs[(UO_2)(HAs_2O_7)]$ (**2**), β-$Cs[(UO_2)(HAs_2O_7)]$ (**3**), $Cs[(UO_2)(HAs_2O_7)]\cdot 0.17H_2O$ (**4**), respectively. All the title compounds were chemically and structurally characterized. The structural and topological relationships as well as the influence of extreme conditions on possible phase formations were discussed.

Experimental Section

Caution! *The $UO_2(NO_3)_2\cdot 6H_2O$ used in this study contained depleted uranium; nevertheless the standard precautions for handling radioactive materials were obeyed.*

Syntheses

Uranyl nitrate $UO_2(NO_3)_2\cdot 6H_2O$ (International Bioanalytical Industries, Inc.), arsenic(III) oxide As_2O_3 (Alfa-Aesar, 97%) and caesium nitrate $CsNO_3$ (Alfa-Aesar, 99.9%) were all used as received. In all experiments, UO_3 was taken as the initial reactant. UO_3 was prepared by rapidly heating up $UO_2(NO_3)_2\cdot 6H_2O$ powder to 450 °C for 4 hours.

The same synthetic procedure was used for all four compounds. The initial finely grounded mixture of $CsNO_3$, As_2O_3 and UO_3 with a corresponding molar ratio was ground thoroughly in an agate mortar, and then inserted into a platinum capsule which was closed with an impulse micro welding device (Lampert PUK U4). The capsule was then placed in a ½´´ high-pressure assembly, which was inserted in a piston cylinder module of a Voggenreiter LP 1000-540/50 installed at IEK-6, Forschungszentrum Jülich. The initial molar ratios of Cs : As^{III} : U for the syntheses are equal to 2 : 3 : 1, 2 : 6 : 1, 2 : 10 : 1, and 0.75 : 1.75 : 1 for the compounds **1**, **2**, **3**, and **4**, respectively. The exact masses of used reagents are given in Table SI1. The whole synthesis procedure was performed at a pressure of 3 GPa. The capsule with the reaction mixture was heated to 900 °C at a heating rate of 100 °C/min and then slowly cooled down to room temperature at a specific cooling rate, which is 0.5, 0.55, 0.5, and 0.3 °C/min for compound **1**, **2**, **3** and **4**, respectively. The capsules were then broken and yellow greenish crystals of compound **1** and light yellow crystals of compounds **2**, **3**, and **4** were isolated from a bulk reaction product. Based on the U, the average yield was around 80%, 40%, 20%, and 10% for the synthesis of compound **1**, **2**, **3** and **4**, respectively. The by-products of the syntheses of compounds **2**, **3**, and **4** are crystals of compound **1** and amorphous phases.

Interesting is that compound **1** can also be obtained from ambient pressure, high temperature solid state reaction. The experimental details can be found in the supporting information (SI).

Single Crystal X-ray Diffraction

Single crystal X-ray diffraction data were collected at room-temperature on a SuperNova (Agilent) single crystal diffractometer using monochromatic $Mo\ K_{\bar{\alpha}}$ radiation (λ = 0.71073 Å). Single crystals were mounted on a glass fiber with epoxy glue. The data were collected using a narrow-frame method with the ω-scan mode. The data were integrated using the CrysAlis^{Pro} program, and the intensities were corrected for Lorentz polarization and absorption attributable to the variation in the path length through the detector faceplate. Absorption correction based on the Multiscan technique was applied. The structures were solved by direct methods using SHELXS-2014[34] and then refined by full-matrix least-squares refinements on F^2 with SHELXL-2014, being part of the software suite WinGX v1.80.05.[35] All of the structures were verified using the ADDSYM algorithm from the program PLATON, and no higher symmetries were found. Relevant crystallographic data and details of the experimental conditions for all the four structures are summarized in Table 1. All crystal chemical calculations were performed using the TOPOS software package (http://topos.samsu.ru).[36, 37]

Elemental Analysis

The chemical compositions were analysed using a scanning electron microscope combined with an energy-dispersive spectroscope (SEM/EDS) (FEG, Quanta 200 F, 60 Pa, 30kV). The instrument is equipped with an Apollo Silicon Drift Detector (SDD) from EDAX. The accuracy of the EDX measurements was verified using individual standards for all measured elements. The measurements were carried out using single crystals (Fig. SI1) and they do confirm the chemical compositions that were found during structure refinements. The results of the EDX elemental analysis (Table SI2) are in good agreement with those used for the single crystal X-ray diffraction studies.

Bond-Valence Analysis

Bond-valence sums (BVS) for all atom positions in the four caesium uranium arsenate phases were calculated, and the results are given in the Supporting Information (Table SI3). The bond-valence parameters provided by Burns[38] were used to calculate the U atom and bond-valence parameters provided by Brown and O'Keeffe[39,40] were used to calculate the As and Cs atom. The BVS for all atoms are coincident with their expected formal valence. Proton positions could not be determined in the X-ray studies. Therefore, the presence of OH− groups in the compounds **2**, **3**, and **4**, respectively, was deduced from the calculation of bond valence sums (BVS).

Raman Studies

Unpolarised Raman spectra were recorded with a Horiba LabRAM HR spectrometer using a peltier cooled multi-channel CCD detector. An objective with a 50× magnification was linked to the spectrometer allowing the analysis of samples as small as 2 µm in diameter. All the samples were in the form of single crystals. The incident radiation was produced by a He–Ne laser at a power of 17 mW (λ = 632.81 nm). The focal length of the spectrometer was 800 mm and a 1800 gr/mm grating was used. The spectral resolution was around 1 cm^{-1} with a slit of 100 µm. Spectra were recorded in the range 100 – 1100 cm^{-1}.

Results and Discussion

Synthesis and Chemical Compositions

In our previous work, we were able to obtain the first mixed valence thorium arsenite-arsenate compound, $Th(As^{III}_4As^{V}_4O_{18})$[24], of the Th^{4+} – As^{3+} system by providing enough As(III) among the

starting reactant. In this work, considering that U is more oxidizing compared to Th, UO_3 was taken as an initial reagent with the aim of less nitrate anions participating in the reaction process. Although we used As_2O_3 as the initial reagent, the resulting compounds contained only arsenic in +5 oxidation states, which could be due to the presence of air in the initial powder and the oxidizing influence of U.[41] As the reactions were performed in sealed capsules, OH^- groups and H_2O molecules were observed in three of the resulting HT/HP phases. For the high-temperature reactions at ambient pressure, protons and water molecules could not be prevented from dispersing into the atmosphere.

The application of pressure enabled the synthesis of materials, which would have never been obtained by ambient pressure high temperature solid state reactions. The phases obtained from HT/HP reactions can keep structural features of materials obtained from both high temperature solid state reactions and solutions/solvothermal methods. In this study we synthesized uranium phases with structural fragments previously observed only in materials from HT solid state reactions and OH groups which are typically observed only in uranyl materials obtained from water solution.

The presence of heavy elements in the structures of all the obtained compounds was confirmed by EDX elemental analysis (Table SI2) and the element ratios agree well with the SC XRD results. The presence of OH^- groups in compounds **2**, **3,** and **4** has been confirmed by bond valence sum (BVS) calculations (Table SI3). The obviously lower BVS values for certain oxygen atoms with about 1.0 v.u. are indicators for the presence of protons. These atoms were not detected by X-ray diffraction experiments and were added according to H atoms BVS donation on the oxygen atoms within OH^- groups. The presence of water molecules in compound **4** is also confirmed by BVS calculations (the valence unit is around 0.26 v.u. for OW1 (H_2O); see tables SI2 of the Supporting Information).

Structure Description

$Cs_2[(UO_2)(As_2O_7)]$ (**1**) crystallizes in the centrosymmetric orthorhombic space group *Pmmn* (Table 1) and is based upon $[(UO_2)(As_2O_7)]^{2-}$ 2D layered motifs (Fig. 1a). Uranium forms short bonds with two O atoms in order to construct linear uranyl groups UO_2^{2+}. Four longer U – O bonds are completing the square bipyramidal coordination geometry of uranium in the equatorial plane. The average U=O bond length in UO_2^{2+} is 1.78 Å and the U–O bond distances are in the range from 2.286 (3) to 2.291(3) Å. Two symmetrically independent arsenic atoms, with site-symmetry C_s, form a As_2O_7 dimer. The As–O bond length ranges from 1.626(5) to 1.678(3) Å and from 1.751(3) to 1.759(3) Å for the terminal and the bridging O atoms, respectively. According to the classification given by Serezhkin et al.[42] and Vologzhanina et al.[43], ligands can be categorized into a coordination scheme by the number of donor oxygen atoms coordinating a U atom (or other metal centers): M, B, T, Q, etc. for mono-, bi-, tri-, tetradentate ligands. The superscript numbers equal to the amount of U atoms connected through one, two, three, etc. donor O atoms, respectively.

Table 1. Crystallographic data of $Cs_2[(UO_2)(As_2O_7)]$ (**1**), α-$Cs[(UO_2)(HAs_2O_7)]$ (**2**), β-$Cs[(UO_2)(HAs_2O_7)]$ (**3**), and $Cs[(UO_2)(HAs_2O_7)]\cdot 0.17H_2O$ (**4**), respectively.

Compound	**1**	**2**	**3**	**4**
Space group	*Pmmn*	$P\bar{1}$	*C2/m*	*P*1
a /Å	13.0174(3)	6.8433(6)	21.269(5)	6.7984(2)
b /Å	13.2673(2)	9.8898(9)	11.812(5)	9.8513(3)
c /Å	6.1849(2)	13.7565(14)	10.735(5)	20.5988(6)
α /°	90	72.363(9)	90	77.494(2)
β /°	90	88.882(8)	100.110(5)	82.150(2)
γ /°	90	83.831(7)	90	84.030(2)
V /Å^3	1068.17(5)	882.04(14)	2655.1(18)	1330.25(7)
ρ_{calc} /g cm^{-3}	4.960	5.006	4.989	4.999
Z	4	4	12	6
λ /Å	0.71073	0.71073	0.71073	0.71073
F(000)	1360	1140	3420	1718
$R(F)$ for $F_0^2 > 2\sigma(F_0^2)$[a]	0.0248	0.0515	0.0579	0.0351
$wR_2(F_0^2)$[b]	0.1165	0.1212	0.0942	0.1062

[a] $R(F) = \Sigma||F_0| - |F_c||/\Sigma|F_0|$. [b] $R(F_0^2) = [\Sigma w(F_0^2 - F_c^2)^2/\Sigma w(F_0^2)^2]^{1/2}$.

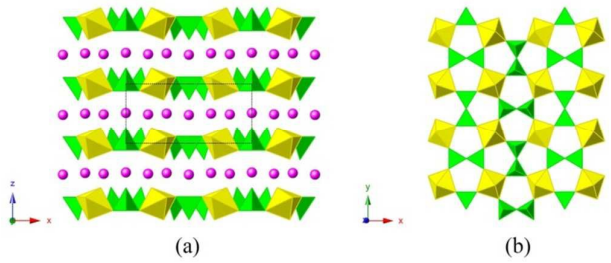

***Figure 1**. (a) Structural fragments of **1**. (b) Schematic representation of the layered structure in **1**. U and As coordination polyhedra are shown in yellow or green, respectively; Cs atoms are in magenta. O atoms are omitted for clarity.*

Based on this, the arsenate anions in **1** can be assigned to Q^4 coordination type, because each UO_6 polyhedron coordinated to four As_2O_7 groups to form a $[(UO_2)(As_2O_7)]^{2-}$ layer (Fig. 1b). The Cs atoms, which serve for charge balancing, are located within the interlayer in order to connect the layers to a 3D assembly. The Cs atoms have a ten-fold oxygen coordination with Cs–O bond distances ranging from 3.020(5) to 3.789(3) Å. $Cs_2[(UO_2)(As_2O_7)]$ is isostructural to the known structure $A_2[(UO_2)(P_2O_7)]$ (A = Rb, Cs)[44] and $K_2[(UO_2)(As_2O_7)]$[45], where uranyl square bipyramids share equatorial vertices with pyrophosphate or pyroarsenate groups to form 2D sheets. In this work, $Cs_2[(UO_2)(As_2O_7)]$ can be taken as the stable ambient pressure phase, which can also be obtained at extreme pressure conditions.

α-Cs[$(UO_2)(HAs_2O_7)$] (**2**) crystallizes in the triclinic space group $P\bar{1}$ (Table 1) and is also based upon the already mentioned layered motif (Fig. 2a). It contains two symmetrically independent uranium sites, which form linear uranyl groups UO_2^{2+} with two short U=O bonds and five longer bonds in the equatorial plane, resulting in a pentagonal bipyramidal coordination geometry UO_7. The average U=O bond length in UO_2^{2+} is 1.77 Å and the equatorial U–O bond distances fall in the range from 2.325(12) to 2.513(11) Å. Arsenic atoms occupy four C_1 sites in the structure of **2** and form a HAs_2O_7 dimer. The As–O bond distances are in the ranges from 1.635(11) to 1.698(11) Å and from 1.731(11) to 1.795(12) Å for the terminal and bridging O atoms, respectively. According to the BVS calculation results (Table SI3b), the valence unit for O6, O9, O13, and O18 is 1.36, 1.24, 1.48, and 1.41 v.u., which is an evidence of participation of these atoms in OH groups. Two UO_7 pentagonal bipyramids share equatorial edges forming dimers, that are six-fold coordinated to HAs_2O_7 hydrated pyroarsenate groups. The resulting layers $[(UO_2)(HAs_2O_7)]^-$ exhibit two geometrical forms A and A' in the structure of **2** (Fig. 2b, c) with a (…A/A'/A/A'…) sequence (Fig. 2a). Layer A can be converted to layer A' by the application of the inversion center. In Fig. 2b and 2c, the up and down orientation of arsenate tetrahedra within the layers A and A' are shown with light blue (up) and green (down) colours. From these figures one can clearly see that the layers A and A' are topologically identical but geometrically isomeric. HAs_2O_7 dimers show two types of coordination, where the first one is of Q^4 type and the second one is of Q^{22} type according to the coordination type classification given in ref 42, 43. Two independent Cs sites are located within the interlayer space and serve, together with the hydrogen atoms from the OH^- groups, as charge balancing cations and for the connection of the layers into 3D assemblies. The Cs1 atom shows an eleven-fold oxygen coordination with Cs–O bond distances ranging from 3.089(11) to 3.664(11) Å. The Cs2 atom is ten-fold coordinated with bond lengths ranging from 3.110(11) to 3.694(12) Å.

β-Cs[$(UO_2)(HAs_2O_7)$] (**3**) crystallizes in the monoclinic space group *C2/m* (Table 1). Compound **3** is a polymorphic modification of compound **2**, with a triple unit cell volume and a dramatic change of the structure. It is based upon the complex 3D framework which makes it significantly different from that of **2** (Fig. 3a) because the latter is based upon a 2D motif (Fig. 2a). Uranium atoms occupy two crystallographically independent sites in **3**, showing two types of coordination environment, namely UO_7 and UO_6. Each uranium atom forms short bonds with two O atoms to form linear uranyl groups UO_2^{2+}. For UO_6, four longer bonds with O atoms in the equatorial plane complete the tetragonal bipyramidal coordination geometry. The average U=O bond length in UO_2^{2+} is 1.77 Å and the U–O bond length ranges from 2.226(11) Å to 2.33(2) Å. For UO_7, the average U=O bond length in UO_2^{2+} is 1.78 Å and the equatorial U–O bond distances range from 2.301(10) Å to 2.432(7) Å. Three crystallographic As sites, with site-symmetry C_1, form HAs_2O_7 dimers.

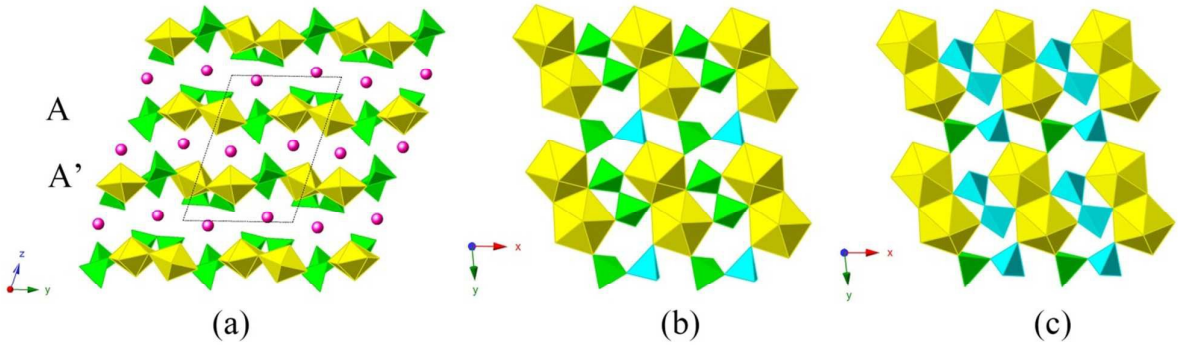

***Figure 2**. (a) Structural fragments of compound **2** with an outline of the unit cell. (b) Schematic representation of layer A and (c) layer A' in compound **2**, respectively. U coordination polyhedra are shown in yellow colour. In Fig. 2a, the As coordination polyhedra are green. Cs atoms are in magenta. O atoms are omitted for clarity. In Fig. 2b and 2c, the "up" and "down" geometric orientation of As tetrahedra are shown in light blue and green, respectively.*

The As–O bond distances are in the range from 1.49(2) to 1.815(7) Å. This unusual bond length is due to the disorder of the O14A and the O15A position, respectively. The local coordination environment for U1, U2 and As3 atoms is given in Fig. SI2. UO_7 pentagonal polyhedra share vertices with the arsenate dimer and form the uranyl arsenate 2D sheet. The UO_6 polyhedra in the interlayer region share four equatorial vertices with tetrahedra of HAs_2O_7, linking the structures into the 3D $[(UO_2)(HAs_2O_7)]^-$ framework (Fig. 3a). The Cs atoms are located within the free space of the 3D framework and serve together with hydrogen atoms from different OH groups for charge balancing. Cs1 and Cs2 atoms reveal an eleven-fold oxygen coordination with Cs–O bond distances ranging from 3.223(15) to 3.605(11) Å. The Cs3 atom is twelve-fold coordinated to oxygen with bond lengths ranging from 3.235(9) to 3.598(8) Å. The HAs_2O_7 dimers consisting of As1 and As2 demonstrate a Q^4 coordination mode and the As3-containing one is G^6 coordinated. According to the BVS calculation results (Table SI3c), the valence sum for O4 and O6 is 1.26 and 1.49 v.u., respectively. This is an indication for the presence of a hydrogen atom and OH with mentioned oxygen atoms. The other OH^- groups cannot be detected due to the partial occupation of O2 and O11 sites and the disorder on the O1, O14, and O15 positions, respectively.

The polymorphic modifications of $Cs[(UO_2)(HAs_2O_7)]$ are quite different in their structures but surprisingly have a very similar molar volume. It is about 220 $Å^3$ for α-$Cs[(UO_2)(HAs_2O_7)]$ (**2**) and about 221 $Å^3$ for β-$Cs[(UO_2)(HAs_2O_7)]$ (**3**). Based only on the volume comparison, it is not possible to define which phase is the low/high temperature polymorph. However, we could propose that **3**, a phase with higher symmetry, is a high temperature beta polymorph. Of course, the experimental condition is a key factor for the stabilization of both phases' modifications. In this work, both polymorphs were obtained by similar synthesis procedures using different starting molar ratios of Cs : As^{III} : U equal 2 : 6 : 1 and 2 : 10 : 1 for compounds **2** and **3**, respectively. Thus, more As^{III} was used for the flux for the synthesis of β-$Cs[(UO_2)(HAs_2O_7)]$ compared to α-$Cs[(UO_2)(HAs_2O_7)]$. Speculatively, it may lead to the crystallization of the beta modification in a melted flux because of the large excess of As_2O_3/As_2O_5, where the lack of such flux changes the structure to the layered alpha phase.

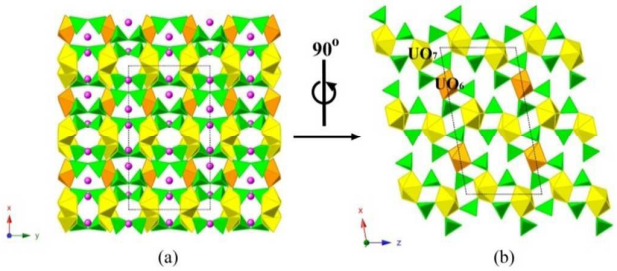

***Figure 3**. (a) Structural fragments of compound **3** (a) along z- axis, (b) along y- axis. UO_7, UO_6 and As coordination polyhedra are shown in yellow, orange and green, respectively; In Fig. 3a, Cs atoms are in magenta. O atoms are omitted for clarity. In Fig. 3b, Cs and O atoms are omitted for clarity.*

The compound **$Cs[(UO_2)(HAs_2O_7)]\cdot 0.17H_2O$** (**4**) crystallizes in the non-centrosymmetric triclinic space group *P*1 (Table 1) and is also based on a layered motif (Fig. 4a), which makes it quite similar to that of **2**. The coordination polyhedron of uranium is also the UO_7 pentagonal bipyramid. The average U=O bond length in UO_2^{2+} is 1.76 Å and the equatorial U–O ranges from 2.297(15) Å to 2.515(13) Å. Twelve crystallographic As sites, with site-symmetry C_1, form HAs_2O_7 dimers. The As–O bond distances are in the range from 1.617(16) to 1.710(13) Å and from 1.728(14) to 1.806(14) Å for the terminal and bridging O atoms, respectively. Here, for the coordination types of HAs_2O_7 arsenate anions, three are of Q^4 type and the other three are of Q^{22} type. The Cs atoms are within the interlayer space, where they are balancing the negative charges of the layers and providing connections of the layers into the 3D

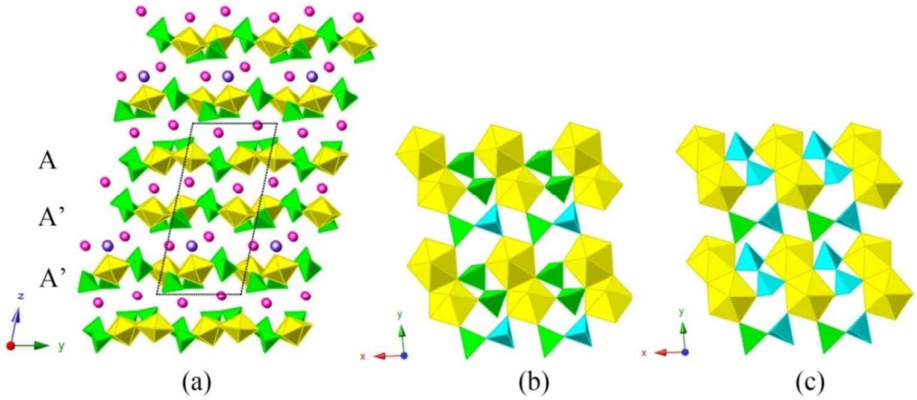

***Figure 4**. (a) Structural fragments of compound **4** with an outline of the unit cell. (b) Schematic representation of layer A and layer A'(c) in compound **4**, respectively. The colour assignment is identical to that in Fig. 2. The water molecules are shown as mauve coloured spheres.*

assembly. The structures of the layers in **4** are identical to that of the layers in compound **2**. In Fig. 4b and c, the layer A and layer A' are shown parallel to the z axis, and the up and down orientation of the arsenate tetrahedra is highlighted by light blue and green colours, respectively. The topologically identical but geometrically isomeric layers A and A' are arranged with a sequence (…A/A'/A'A/A'/A'…) in the structure of **4**. The water molecules are located between two neighbouring A'-type layers only. The presence of water molecules in the interlayer space does not only change the Cs coordination, but also the hydrogen bonds (h.b.) system and thereby the configuration of the layers comparably to that in the structure of **2**. The possible h.b. in structures **2** and **4** within the interlayer space is shown in Fig. SI3. In this figure it can also be noticed that the additional H_2O molecule in structure **4** changes the layers sequence from (A/A') for structure **2** to (A/A'/A') in structure **4**. There are six crystallographic Cs sites, with site-symmetry C_1, located within the interlayer space to form the $Cs1O_{12}$, $Cs2O_{11}$, $Cs3O_{11}$, $Cs4O_{12}$, $Cs5O_{11}$, and $Cs6O_{10}$ polyhedra. The Cs–O bond distances range from 3.043(15) to 3.808(15) Å. The Cs4 and Cs6 atoms are connected to a single water molecule each, and to 11 or 9 O atoms, respectively.

Topological Analysis and Polymorphism

It has already been mentioned above that the layers A and A' in compounds **2** and **4** are topologically identical, but geometrically isomeric. In Fig. 5, the differences between the layers were identified by the orientation of the AsO_4 tetrahedron (white dot) with symbols **u** (up) and **d** (down). Fig. 5a e.g. shows a black-and-white graph of layer A. All HAs_2O_7 groups are four-fold coordinated to an U atom with coordination type Q^4 and Q^{22}, and thus, there are two O_{Cs} atoms connected to every Cs atom in each HAs_2O_7 group. Therefore, O_{Cs} atoms determine the orientation of the AsO_4 tetrahedra. As a result one gets two geometrically isomeric layers A and A' in compound **2** and **4**, as illustrated in detail in Fig. 5b-5c.

Though the composition of compounds **1**, **2**, and **4** is very similar, the presence of OH groups in **2** and **4** leads to a change of the coordination modes of the hydro pyroarsenate groups. In **1**, a single crystallographic site of the hydro pyroarsenate anions corresponds to a Q^4 coordination type. In **2**, there are two crystallographic types of HAs_2O_7 groups, either of Q^4 or Q^{22} coordination type. It is noteworthy that the presence of OH groups in the structure of **2** does not change the amount of donor atoms in the HAs_2O_7 groups as could have been expected. The structure of **4** is more complicated compared to **2**, because it contains more crystallographically independent atoms (six independent U atoms in **4** vs. two in **2**), but its structure closely relates to **2**. Indeed, there are six crystallographically independent HAs_2O_7 groups equally corresponding to the Q^4 and Q^{22} coordination types. To compare the structures of **1**, **2**, and **4** we built the cation graphs and simplified nets of the layers in these structures. In those three structures, each HAs_2O_7 group is bound to four UO_2 groups and each uranyl group is bound to four pyroarsenate groups. Due to the influence of the coordination type to the connectivity, only layers of **2** and **4** are isoreticular (Fig. 6a), because both structures contain Q^4 and Q^{22} HAs_2O_7 groups with a 1 : 1 ratio. The only difference in composition of **2** and **4** is an additional small amount of water in **4** (0.17 per formula unit according to the SC XRD data) being located between the two layers A'. This difference leads to distortions in the layers resulting in three crystallographically independent layers.

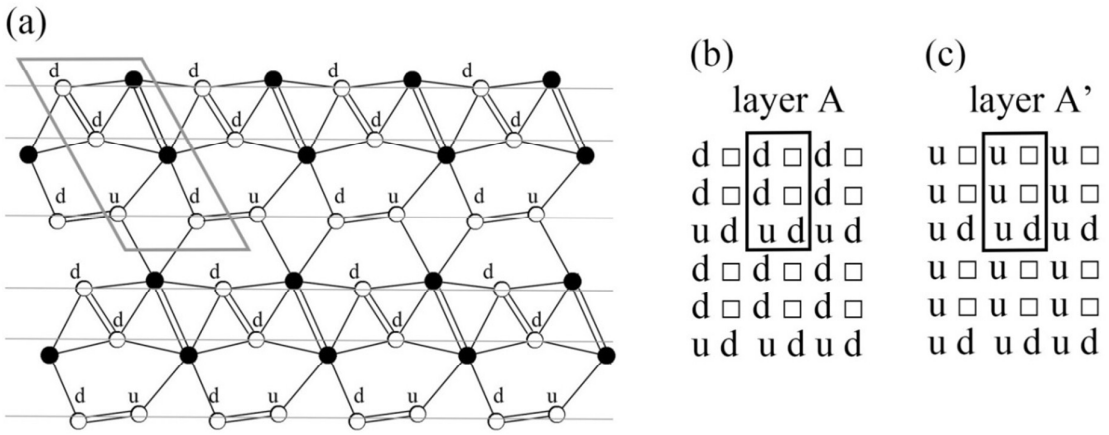

***Figure 5**. (a) Black-and-white graph with **u**, **d**, and □ symbols written close to the black vertices for the layer A in compound **2** and **4**. (b, c) Tables for topologically identical, but geometrically isomeric layers A and A', respectively. Bold lines indicate the orientation matrices of AsO_4 tetrahedra. Black and white nodes correspond to U and As atoms, respectively. Edge shared atoms are connected by double lines.*

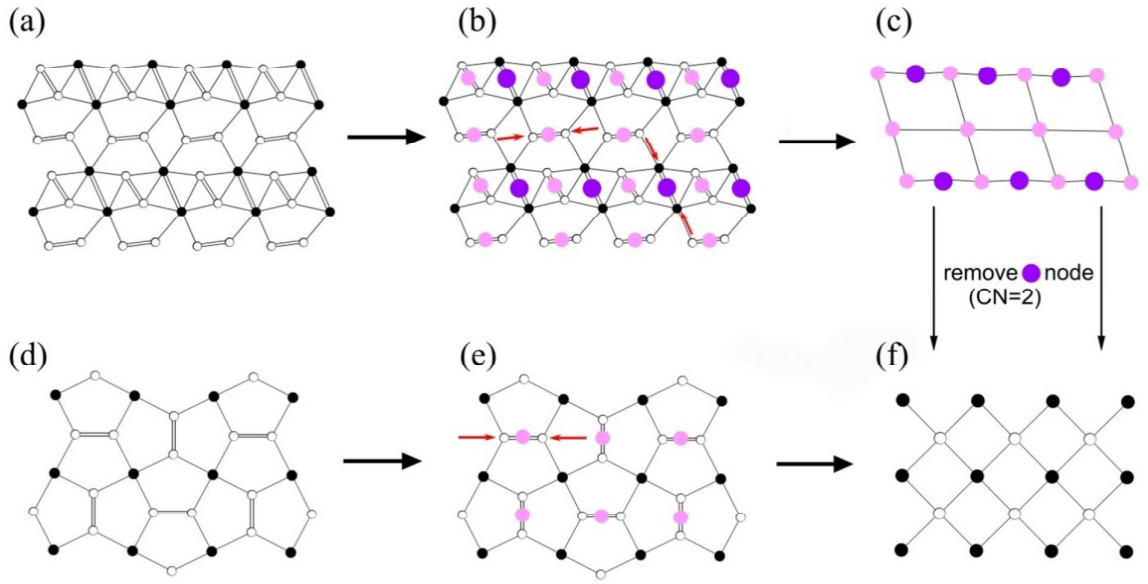

Figure 6. *(a) Black-and-white graph of layer A in structures **2** and **4**, (b) contracting the edge shared dots (white and black, respectively) into one node (pink and purple, respectively), (c) new coloured-nodes representing the net simplified from layer A, (d) black-and-white graph of layers in structure **1**, (e) HAs_2O_7 are contracted into a node (pink), (f) the layer in the autunite structure type[46] with stoichiometric formula $[(UO_2)(TO_4)]$ (**T** = As or P). Black and white nodes correspond to U and As atoms, respectively. Pink and purple nodes are the contracted ones.*

Further simplification leads to 2D underlying nets shown in Figure 6. The black-and-white graph of layer A in compound **2** and **4**, of the layer in compound **1** and the layer in autunite-type structures[46] is shown in Fig. 6a, 6d and 6f, respectively. During the simplification, all the HAs_2O_7 groups are contracted into one node (pink) in order to save their connectivity to uranium atoms (Fig. 6b, e). The edge sharing U dots in Fig. 6b are also contracted into one node (purple). In Fig. 6c, the purple node with coordination number (CN = 2) will be removed to simplify the underlying net, but simultaneously avoiding to change the topology type. Finally, the resulting simplified nets of structures **1**, **2**, and **4** are common **sql** nets (Fig. 6f) which can be found in autunite-like layered compounds. It is interesting to note that in the autunite layers, $[UO_2PO_4]^-$, the phosphate anions correspond to the Q^4 coordination type. Therefore, dimerization of arsenate groups in the structures of **1**, **2**, **4** does not significantly change the topology of the compounds compared to autunite-like As-containing compounds, which are the most common uranium phosphate/arsenate minerals.

Raman Analysis

The Raman spectra of $Cs_2[(UO_2)(As_2O_7)]$ (**1**), α-$Cs[(UO_2)(HAs_2O_7)]$ (**2**), β-$Cs[(UO_2)(HAs_2O_7)]$ (**3**), and $Cs[(UO_2)(HAs_2O_7)]\cdot 0.17H_2O$ (**4**) are presented in Fig. 7. All measured modes are below 1000 cm^{-1}. Surprisingly, no vibrations for OH^- groups and water molecules were detected in the range from 1000 to 4000 cm^{-1}. But the spectra contain a large number of bands that belong to three main regions.

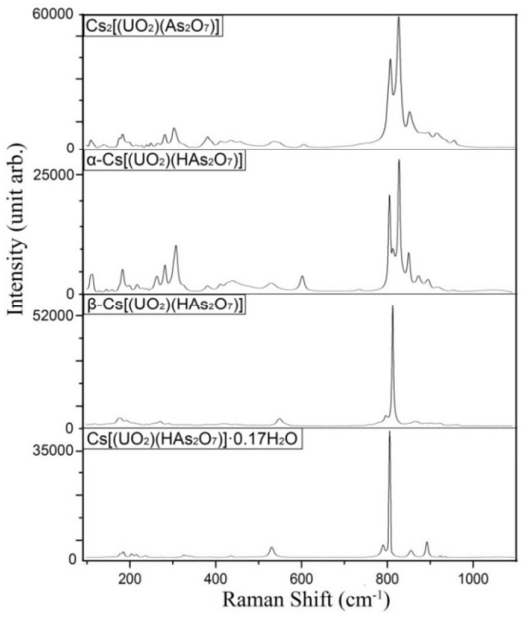

Figure 7. *Raman spectra of $Cs_2[(UO_2)(As_2O_7)]$ (**1**), α-$Cs[(UO_2)(HAs_2O_7)]$ (**2**), β-$Cs[(UO_2)(HAs_2O_7)]$ (**3**), and $Cs[(UO_2)(HAs_2O_7)]\cdot 0.17H_2O$ (**4**), respectively.*

Table 2. Determined Raman modes (cm^{-1}) and some proposed band assignments for $Cs_2[(UO_2)(As_2O_7)]$ (**1**), α-$Cs[(UO_2)(HAs_2O_7)]$ (**2**), β-$Cs[(UO_2)(HAs_2O_7)]$ (**3**), and $Cs[(UO_2)(HAs_2O_7)]\cdot 0.17H_2O$ (**4**), respectively.

1		2		3		4	
962w		961w		969w		938w	
940w		926w		958w		928w	
922w		902w	$\nu_3(UO_2)$	931w		896m	$\nu_3(UO_2)$
902w	$\nu_3(UO_2)$	880w		920w		859m	ν_3
888w		857m	ν_3	910w			
865w				898w			
857m	ν_3			892w	$\nu_3(UO_2)$		
				879w	ν_3		
				870w			
				858w			
832s	$\nu_1(UO_2)$	834s	$\nu_1(UO_2)$	820s	$\nu_1(UO_2)$	818w	
822m		819m		803m	ν_1	815w	
812s	ν_1	811s	ν_1	787w		809s	$\nu_1(UO_2)$
807m		740w		767w		804w	
777w						794sm	ν_1
610w		606w		569sh		533m	
553w		565w		554m		439w	ν_4
537w	ν_4	533w	ν_4	493w	ν_4		
467w		474w		458w			
461w		459w		449w			
438w		441w		431w			
415w		427w		419w			
		414w		405w			
		404w					
393w		391w		381w		344w	
384w		383w		341w		336w	
380w		376w		326w	ν_2	328w	ν_2
324w		324w					
310w		310m	ν_2				
304m	ν_2	303w					
296w		298w		293w		274w	
284w		283m		274m		238w	
267w		264m		263w		217w	
251w		241w		258sh		206w	
242w	$\nu_2(UO_2)$,	231w	$\nu_2(UO_2)$,	243w	$\nu_2(UO_2)$,	187w	$\nu_2(UO_2)$,
228w	$\nu_4(UO_2)$, and	218w	$\nu_4(UO_2)$, and	222w	$\nu_4(UO_2)$, and	180sh	$\nu_4(UO_2)$, and
217w	lattice	200w	lattice	211w	lattice	159w	lattice
200w	vibration	192sh	vibration	204sh	vibration		vibration
192w		184m		195m			
185w		175sh		184sh			
177sh		159w		177m			
160w		146w		161w			
141w		129w		149w			
137w		113w		143w			
128w		108w		120w			
114w							
109w							
100w							

The accuracy of all values is assumed to be ±1 cm^{-1}. Note that the band assignments were carried out according to the previous literature data upon both solid-state and aqueous solution of AsO_4^{3-} and UO_2^{2+} groups. s = strong, m = medium, w = weak, sh = shoulder. The assignment for the uranyl group is shown as $\nu_n(UO_2)$, while for the assignment of the arsenate group, ν_n (n= 1, 2, 3, 4) is used.

According to literature data[47-49], the proposed band assignments of the UO_2 and the arsenate groups are summarized in Table 2. The first main region can be identified in the range from 700 to 1000 cm^{-1}, and can be assigned to the symmetric and anti-symmetric stretching vibrations of the uranyl and the arsenate groups, ν_1 and ν_3, respectively. There is the difficulty that both the ν_1 bands of AsO_4 and UO_2^{2+} are found at the same spectral positions making interpretation by vibrational spectroscopy a challenge[50-52]. The second and the third main region also cannot be distinguished unambiguously without theoretical calculations of the spectra due to overlapping peaks. However, the symmetric and anti-symmetric bending vibrations of UO_2^{2+}, ν_2 and ν_4, can be found below 300 cm^{-1}, whereas the respective bending modes of AsO_4 are assumed between 300 and about 540 cm^{-1} (see Table 2 for details).

Conclusions

Using a high-temperature (900 °C) and high-pressure (3 GPa) facility, we synthesized a new family of uranyl arsenates, $Cs_2[(UO_2)(As_2O_7)]$ (**1**), α-$Cs[(UO_2)(HAs_2O_7)]$ (**2**), β-$Cs[(UO_2)(HAs_2O_7)]$ (**3**), and $Cs[(UO_2)(HAs_2O_7)]\cdot 0.17H_2O$ (**4**), respectively. Compounds **2**, **3**, and **4** are the first examples of uranyl arsenates obtained under extreme conditions. The structures of compound **1**, **2**, and **4** are based upon 2D layered motifs. Compound 1 can also be synthesized at ambient pressure by a high temperature solid state reaction. The uranyl arsenate layers A and A' in compounds **2** and **4** are topologically identical, but geometrically isomeric layers. Despite the presence of pyroarsenate groups, the structures of compounds **1**, **2**, and **4** and their sheet anion topologies can be simplified to that of autunite-type sheets. Our work reveals that the uranyl arsenate sheet of the ambient pressure phase **1** can be directly transformed to that of the autunite-type sheet by contracting the As_2O_7 group. However, more simplification processes are required when the uranyl arsenate sheet of compound **2** and **4** are transformed to that of the autunite-type sheet. Among all four structures, no significant changes appear in the coordination chemistry of the UO_2^{2+} group. But under the effect of high-pressure, the structures of polymorphs **2** and **3** show great changes, which transformed from a 2D layered motif to a 3D framework. This work demonstrates the significant influence of the synthesis conditions on the formation and the structural properties of the obtained uranium compounds. The sealed capsules allow obtaining of the hydrates and phases with hydroxyl groups at high temperatures. As a result, the internal connectivity and the geometrical diversity of resulting materials is strongly influenced.

Acknowledgements

Authors are grateful to Dr. Martina Klinkenberg (IEK-6, Forschungszentrum Jülich) for her kind help in EDX experiments and Jakob Dellen for his help in Raman spectra collection. We are also grateful to the Helmholtz Association for funding within the VH-NG-815 grant.

References

1.Xiao, B.; Langer, E.; Dellen, J.; Schlenz, H.; Bosbach, D.; Suleimanov, E. V.; Alekseev, E. V., *Inorganic chemistry* **2015,** *54*, 3022-3030.
2.Xiao, B.; Gesing, T. M.; Kegler, P.; Modolo, G.; Bosbach, D.; Schlenz, H.; Suleimanov, E. V.; Alekseev, E. V., *Inorganic chemistry* **2014,** *53*, 3088-3098.
3.Wang, S.; Alekseev, E. V.; Depmeier, W.; Albrecht-Schmitt, T. E., *Chemical Communications* **2011,** *47*, 10874-10885.
4.Burns, P. C., *Reviews in Mineralogy and Geochemistry* **1999,** *38*, 23-90.
5.Ewing, R. C.; Hawthorne, F. C., *The Canadian Mineralogist* **1997,** *35*, 1551-1570.
6.Oelkers, E. H.; Montel, J.-M., *Elements* **2008,** *4*, 113-116.
7.Du Fou de Kerdaniel, E.; Clavier, N.; Dacheux, N.; Terra, O.; Podor, R., *Journal of Nuclear Materials* **2007,** *362*, 451-458.
8.Terra, O.; Dacheux, N.; Audubert, F.; Podor, R., *Journal of Nuclear Materials* **2006,** *352*, 224-232.
9.Ewing, R. C.; Wang, L., *Reviews in Mineralogy and Geochemistry* **2002,** *48*, 673-699.
10.Schlenz, H.; Heuser, J.; Neumann, A.; Schmitz, S.; Bosbach, D., Monazite as a suitable actinide waste form. In *Zeitschrift für Kristallographie - Crystalline Materials*, 2013; Vol. 228, p 113.
11.Alekseev, E. V.; Krivovichev, S. V.; Depmeier, W., *J. Solid State Chem.* **2009,** *182*, 2977-2984.
12.Alekseev, E. V.; Krivovichev, S. V.; Depmeier, W.; Knorr, K., *Zeitschrift für anorganische und allgemeine Chemie* **2008,** *634*, 1527-1532.
13.Wang, S.; Alekseev, E. V.; Diwu, J.; Casey, W. H.; Phillips, B. L.; Depmeier, W.; Albrecht-Schmitt, T. E., *Angew. Chem. Int. Ed.* **2010,** *49*, 1057-1060.
14.Krivovichev, S. V.; Burns, P. C.; Tananaev, I. G., *Structural Chemistry of Inorganic Actinide Compounds*. Elsevier: Amsterdam, 2007.
15.Yu, N.; Klepov, V. V.; Modolo, G.; Bosbach, D.; Suleimanov, E. V.; Gesing, T. M.; Robben, L.; Alekseev, E. V., *Inorganic chemistry* **2014,** *53*, 11231-11241.
16.Bénard, P.; Brandel, V.; Dacheux, N.; Jaulmes, S.; Launay, S.; Lindecker, C.; Genet, M.; Louër, D.; Quarton, M., *Chemistry of Materials* **1996,** *8*, 181-188.
17.Bénard, P.; Louer, D.; Dacheux, N.; Brandel, V.; Genet, M., *Chemistry of Materials* **1994,** *6*, 1049-1058.
18.Yu, N.; Klepov, V. V.; Neumeier, S.; Depmeier, W.; Bosbach, D.; Suleimanov, E. V.; Alekseev, E. V., *European Journal of Inorganic Chemistry* **2015,** *2015*, 1562-1568.
19.Villa, E. M.; Alekseev, E. V.; Depmeier, W.; Albrecht-Schmitt, T. E., *Cryst. Growth Des.* **2013,** *13*, 1721-1729.
20.Yu, N.; Klepov, V. V.; Villa, E. M.; Bosbach, D.; Suleimanov, E. V.; Depmeier, W.; Albrecht-Schmitt, T. E.; Alekseev, E. V., *J. Solid. State. Chem.* **2014,** *215*, 152-159.
21.Yeon, J.; Smith, M. D.; Tapp, J.; Möller, A.; zur Loye, H.-C., *Journal of the American Chemical Society* **2014,** *136*, 3955-3963.
22.Villa, E. M.; Marr, C. J.; Diwu, J.; Alekseev, E. V.; Depmeier, W.; Albrecht-Schmitt, T. E., *Inorganic chemistry* **2013,** *52*, 965-973.
23.Villa, E. M.; Marr, C. J.; Jouffret, L. J.; Alekseev, E. V.; Depmeier, W.; Albrecht-Schmitt, T. E., *Inorganic chemistry* **2012,** *51*, 6548-6558.

24.Yu, N.; Klepov, V. V.; Kegler, P.; Bosbach, D.; Albrecht-Schmitt, T. E.; Alekseev, E. V., *Inorganic chemistry* **2014,** *53*, 8194-8196.
25.Wu, S.; Kowalski, P. M.; Yu, N.; Malcherek, T.; Depmeier, W.; Bosbach, D.; Wang, S.; Suleimanov, E. V.; Albrecht-Schmitt, T. E.; Alekseev, E. V., *Inorganic chemistry* **2014,** *53*, 7650-7660.
26.Alekseev, E. V.; Krivovichev, S. V.; Depmeier, W., *J. Mater. Chem.,* **2009,** *19*, 2583-2587.
27.Wu, S.; Wang, S.; Polinski, M.; Beermann, O.; Kegler, P.; Malcherek, T.; Holzheid, A.; Depmeier, W.; Bosbach, D.; Albrecht-Schmitt, T. E.; Alekseev, E. V., *Inorganic chemistry* **2013,** *52*, 5110-5118.
28.Lai, Y.-H.; Chang, Y.-C.; Wong, T.-F.; Tai, W.-J.; Chang, W.-J.; Lii, K.-H., *Inorganic chemistry* **2013,** *52*, 13639-13643.
29.Chang, Y.-C.; Chang, W.-J.; Boudin, S.; Lii, K.-H., *Inorganic chemistry* **2013,** *52*, 7230-7235.
30.Liu, H.-K.; Ramachandran, E.; Chen, Y.-H.; Chang, W.-J.; Lii, K.-H., *Inorganic chemistry* **2014,** *53*, 9065-9072.
31.Hinteregger, E.; Wurst, K.; Perfler, L.; Kraus, F.; Huppertz, H., *European Journal of Inorganic Chemistry* **2013,** *2013*, 5247-5252.
32.Hinteregger, E.; Hofer, T. S.; Heymann, G.; Perfler, L.; Kraus, F.; Huppertz, H., *Chemistry – A European Journal* **2013,** *19*, 15985-15992.
33.Sweet, L.; Henager, J. C.; Hu, S.; Johnson, T.; Meier, D.; Peper, S.; Schwantes, J., *Investigation of Uranium Polymorphs*. Pacific Northwest National Laboratory: Richland, Washington 99352, 2011.
34.Sheldrick, G. M., *Acta Crystallographica Section A* **2008,** *64*, 112-122.
35.Farrugia, L. J., *Journal of Applied Crystallography* **2012,** *45*, 849-854.
36.V.A. Blatov; V.N. Serezhkin, *Russ. J. Inorg. Chem.,* **2000,** *45*, S105-S222.
37.V.A. Blatov; A. P. Shevchenko; V.N. Serezhkin, *J. Appl. Crystallogr.,* **2000,** *33*, 1193-1193.
38.Burns, P. C., *Can. Miner.,* **1997,** *35*, 1551-1570.
39.Brown, I. D.; Altermatt, D., *Acta Cryst.,* **1985,** *B41*, 244-247.
40.Brese, N. E.; O'Keeffe, M., *Acta Cryst.,* **1991,** *B47*, 192-197.
41.Hoekstra, H. R.; Siegel, S., *Journal of Inorganic and Nuclear Chemistry* **1961,** *18*, 154-165.
42.Serezhkin, V. N.; Vologzhanina, A. V.; Serezhkina, L. B.; Smirnova, E. S.; Grachova, E. V.; Ostrova, P. V.; Antipin, M. Y., *Acta Crystallographica Section B* **2009,** *65*, 45-53.
43.Vologzhanina, A. V.; Serezhkina, L. B.; Neklyudova, N. A.; Serezhkin, V. N., *Inorganica Chimica Acta* **2009,** *362*, 4921-4925.
44.Linde, S. A.; Gorbunova, Y. E.; Lavrov, A. V.; Pobedina, A. B., *Izvestiya Akademii Nauk SSSR, Neorganicheskie Materialy* **1981,** *17*, 1062-1066.
45.Alekseev, E. V.; Krivovichev, S. V.; Depmeier, W., *Z. Anorg. Allg. Chem.,* **2007,** *633*, 1125-1126.
46.Locock, A. J.; Burns, P. C., *American Mineralogist* **2003,** *88*, 240–244.
47.Ray L, F., *Spectrochimica Acta Part A.* **2004,** *60*, 1469–1480.
48.Tossell, J. A., *Geochimica et Cosmochimica Acta,* **1997,** *61*, 1613-1623.
49.Sabine, G.; Johnstony, C. T., J. Colloid. Interf. Sci. **2001**, 234, 204–216.
50.Frost, R.L., Weier, M.L., Adebajo, M.O., Thermochimica Acta **2004**, 419, 119-129.
51.Frost, R.L., Weier, M.L., Spectrochimica Acta **2004**, Part A 60, 2399-2409.
52.Driscoll, R.J.P., Wolverson, D., Mitchels, J.M., Skelton, J.M., Parker, S.C., Molinari, M. Khan, I., Geeson, D., Allen, G.C., RSC Adv. **2014**, 4, 59137-59149.

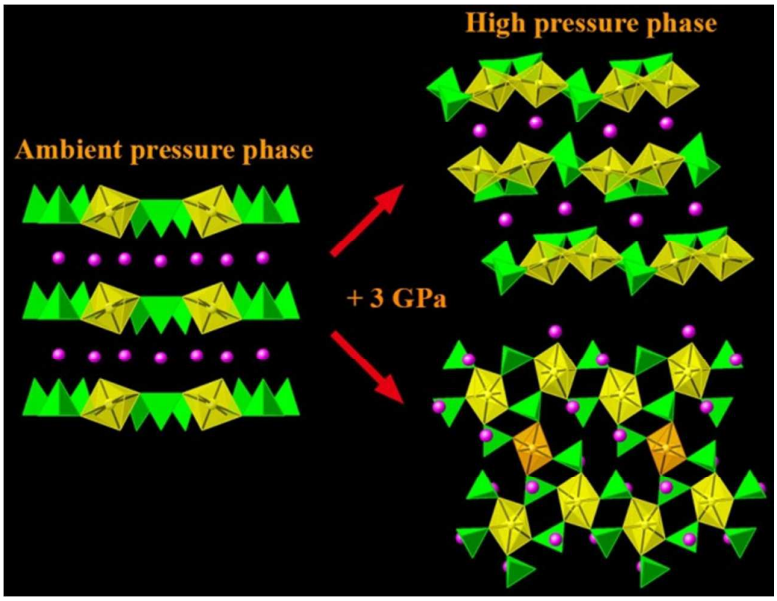

New family of uranium (VI) arsenates was obtained under extreme conditions of pressure and temperature. The high pressure phases demonstrate significant difference in chemical compositions and structural properties.